Applied Environmental Research
- RESEARCH FOR SUSTAINABLE PLANET -

Research Article

Groundwater Recharge and Surface Runoff Modeling Response to Land Use and Land Cover Dynamics in a Mae Wong Watershed of Thailand

Banchongsak Faksomboon[1,*], Pranee Lertkaeo[2], Bunchongsri Phunlao[3]

[1] Faculty of Science and Technology, Environmental Science Program, Kamphaeng Phet Rajabhat University, Thailand
[2] Faculty of Education, Faculty of General Science Program, Kamphaeng Phet Rajabhat University, Thailand
3 Khon Kaen Juvenile and Family Court, Mueang Khon Kaen District, Khon Kaen Province, Thailand

*Correspondence Email: banchongsakf@gmail.com

Abstract

This study aims to develop efficient management strategies and assess the spatiotemporal dynamics of land use and land cover (LULC) on surface runoff modeling response dynamics for the long-term sustainability of watersheds. The soil and water assessment tool (SWAT) model was used to evaluate the LULC dynamics on GRSR in the Mae Wong Watershed (MWW) of Thailand. Using Landsat images, three different LULC maps (2011, 2021, and 2031) were created using the cellular automata markov chain (CA-Markov) model, and TerrSet 2020 geospatial monitoring and modeling software. In the overall MWW, the forestland has undergone deforestation and decreased by 2.10% of the total area and 2.72% of the total area has been transformed into agricultural lands due to human activity and population growth. The soil, LULC, weather, and the digital elevation model (DEM) were all used in the SWAT simulation procedure. To understand the groundwater recharge and surface runoff (GRSR) responses of each hydrologic response units (HRUs), the SWAT model was calibrated and verified using streamflow and the sequential uncertainty fitting (SUFI-2) technique from the SWAT calibration and uncertainty program (SWAT-CUP). The results indicate that there is a good agreement for both the calibration and validation phases of all LULC simulations. The study indicated that groundwater recharge has decreased over the last two decades while surface runoff has increased due to the forest area being converted to agricultural land. Thus, the study can support maximizing water management and strategies for systematically attaining sustainability.

ARTICLE HISTORY

Received: 24 Dec. 2023
Accepted: 20 Jan. 2024
Published: 24 Feb. 2024

KEYWORDS

Hydrological modeling;
Water resources;
Water balance;
LULC management;
SWAT

Introduction

Uncertainties around climate change and changes in LULC dynamically impede land and water supplies, exacerbating the global water crisis. Land and water resources are being threatened by improper exploitation and inadequate management practices, which are transforming the natural landscapes for human use [1]. To effectively manage the available resources, it is necessary to examine the potential implications of LULC change on the hydrologic cycle under both natural and human activity [2–3]. Groundwater is the primary source of fresh water in several climate regions, and its use and management are closely tied to sustainable development goals [4–5]. In contrast, the extensive use of groundwater for home and agricultural reasons negatively affects groundwater recharge and food security in the majority of countries [1–2, 6]. The LULC has a considerably greater impact than climate change. Awareness of the abstraction possibilities of water management requires an understanding of the spatiotemporal variability of groundwater recharge and streamflow [7–8]. While high inter-annual rainfall changes

https://doi.org/10.35762/AER.2024005

put a strain on the availability of surface water, groundwater is a more desirable source of water than surface water. In developing countries, estimating GRSR is challenging because there aren't many sources of pertinent data [8]. Thailand has abundant water and land resources; however, these advantages have had little impact on the growth of the country's economy in regard to increased agricultural output for food security [1], it is being impacted by a variety of environmental concerns. A substantial LULC change has been documented during the previous few decades, primarily due to man-made and natural influences [9–11]. Water stress caused by anthropogenic and natural activities changes ecosystem biodiversity by negatively affecting watershed hydrology. This has a negative impact on the environment's fundamental elements, geomorphologic patterns, the fragmentation of flora and fauna habitats, the loss of biodiversity, and climatic changes. The most important thing is to minimize the effects of LULC change on groundwater recharge. Differences in evapotranspiration, surface runoff, groundwater recharge, and LULC change have an impact on the spatiotemporal scales of land surfaces [1, 12–14]. However, major water stress has been experienced in most developing nations, including Thailand, because of information gaps in the decision-making process. Planning and making use of water resources requires an under-standing of the hydrologic cycle in order to create an appropriate watershed model. In order to address a broad range of environmental issues, watershed models have been employed as a dynamic mechanism, improving the prediction accuracy of estimates [3, 15–16]. A powerful hydrologic model for estimating hydrologic fluxes in addressing water scarcity issues is the SWAT [17]. Multiple ecological processes are integrated into the model to assist management and decision-making scenarios across the globe change through time [3, 5, 18–22].

For watershed management to remain sustainable, using the geographical data and modeling process are crucial to categorize and evaluate the spatiotemporal changes in groundwater recharge [8, 23]. However, while water and food security are major concerns, basic knowledge of the spatiotemporal patterns of LULC change and its impact on GRSR in Thailand is infrequently recognized. Due to significant changes in numerous anthropogenic activities, GRSR is difficult. Furthermore, groundwater recharge could be negatively impacted by sediment deposition if surface runoff is not appropriately controlled because it is the energy source for soil erosion that leads to reservoirs [24]. Therefore, groundwater recharge and surface runoff modeling studies are essential for creating water infrastructure that supports sustainable watershed management techniques in regions with little data. For the sustainable management of water resources, a thorough comprehension of the results and implications of LULC and watershed monitoring systems is required. The SWAT model was effectively used to evaluate the unique effects of LULC variations on GRSR in order to confirm the practicality of predicting streamflow. The study's goal is to ascertain, in situations with limited data, how changes in land use and land cover affect surface runoff and groundwater recharge. This study will help spread strategies for resource development and watershed management that are sustainable.

Methodology

1) Study area

The Mae Wong Watershed (MWW) area is in northern Thailand, between latitudes 99°06′36.05″E and 99°34′51.79″E, and longitudes 16°18′29.82″N and 15°66′31.56″N, covering an area of 199.96 km^2, and is the part of the Ping Watershed (34,499 km^2). It flows from west to east, covering the lower parts of Kamphaeng Phet Province (Figure 1A). The LULC of MWW were classified into 14 classes: cassava, corn, deciduous forest, evergreen forest, field crop, mixed forest, orchard, other, paddy field, pasture, rubber trees, sugarcane, urban or built-over area, and water, respectively (Figure 1B). The land west of the MWW area is predominantly evergreen forest and deciduous forest, of which half of the area is mostly cassava, paddy field, and urban or built-over area, respectively. The total stream flow from the upper to the outlet consists of forests, valleys, and agricultural lands with an urban or built-over area long of approximately 96.39 km. The percentage of the land covered by slope is 0–2 (22.41%), 2–5 (17.10%), 5–12 (16.76%), 12–35 (21.65%), and 22.08% for slopes above 35 percent (Figure 1C). The geological structures are joints in igneous rock and sedimentary and metamorphic rock. The area reveals Tertiary rocks, including Cambrian, Jurassic, Pre-Cambrian, Qua-ternary, Silurian-Devonian, and Triassic, as in Figure 2A. The west MWW consists of high elevation surrounded by mountains with the DEM ranging between 73 and 1,230 mean sea-level (MSL) (Figure 2B), and a contour line ranging between 100 and 1,200 MSL (Figure 2C).

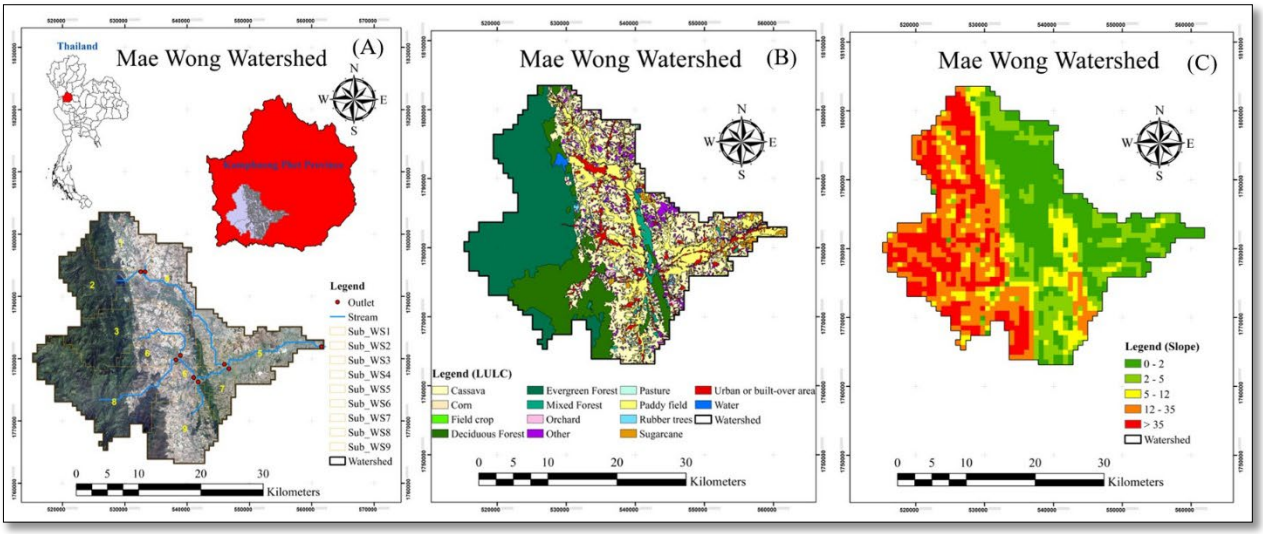

Figure 1 Location (A), LULC (B), and Slope (C) of Mae Wong Watershed.

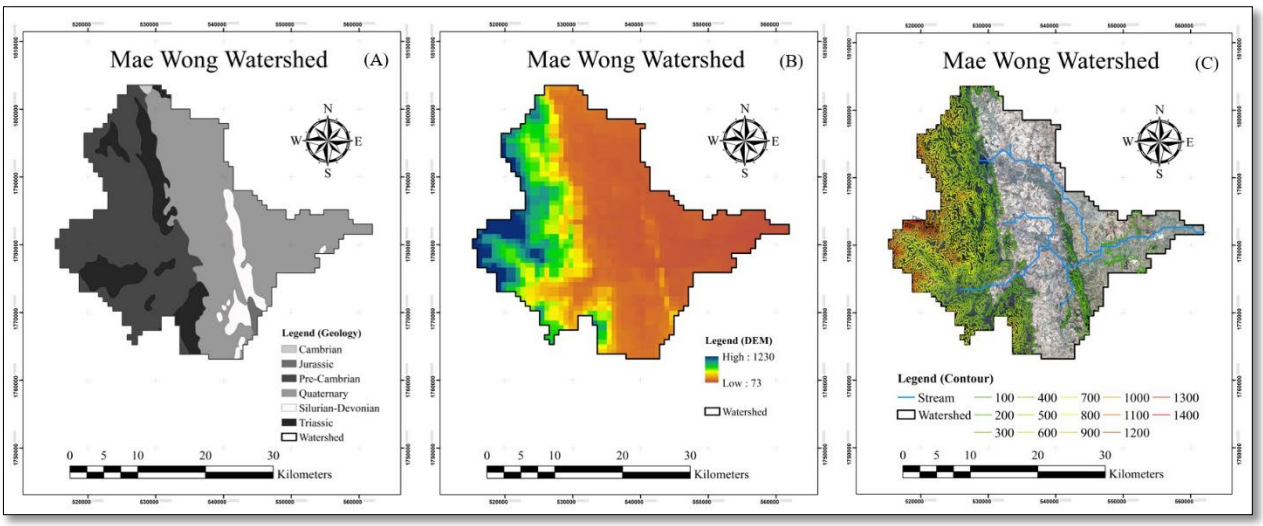

Figure 2 Geology (A), Digital Elevation Model (B), and Contour line (C).

2) The SWAT model

The SWAT model can simulate water management environments since it is continuous, physically based, and The Mae Wong Watershed (MWW) of hydrological and meteorological processes). With easily accessible input data, the model is created to mimic runoff and nutrient losses in order to evaluate management techniques [25]. Typically, the SWAT has been used to assess the effects and implications of LULC change on the hydrology of watersheds [3, 11, 13, 26-27]. It mimics both a shallow unconfined aquifer that provides water to the main-stream and a deep limited aquifer that reaches the sub-watershed [28]. This improves the water balance's accuracy and gives it a strong physical meaning. Additionally, SWAT uses the water balance Equation to mimic the hydrological cycle [28-30], shown in Eq. 1.

$$SW_t = SW_0 + \sum (R_{day} - Q_{surf} - E_a - W_{seep} - Q_{gw}) \quad \text{(Eq. 1)}$$

Eq. 1 SW_t is the final soil water content (mm H_2O), SW_0 is the initial soil water content (mm H_2O), t is the time (days), R_{day} is the amount of precipitation on the day (mm H_2O), Qsurf is the amount of surface runoff on the day (mm H_2O), E_a is the amount of evapotranspiration on the day (mm H_2O), W_{seep} is the amount of percolation and bypass flow exiting the soil profile bottom on the day (mm H_2O), Q_{gw} is the amount of return flow on the day (mm H_2O) [28].

3) Model input data preparation

To simulate hydrologic processes, the SWAT model requires topography, LULC data, soil data, and daily weather data. A lookup table links the input soil map, soil class, and SWAT model database. This study considered LULC changes in the context of this study, Google Earth Engine employed satellite data search images. Landsat 8 images in the year 2011, as in Figure 3A, and 2021 as in Figure 3B, are used to the LULC scenario by 2031, as in Figure 3C. This study used the

supervised classification of the support vector machine (SVM) for the pre-identification of precisely targeted categorization after the images were transferred using the ENVI application and cellular automata markov chain (CA-Markov) model [27]. The images were categorized using supervised classification using maximum likelihood estimation, which produced a pixel-by-pixel land use map of the MWW. As a result, it is thought that the integrated cellular automata markov chain (CA-Markov) model is a capable estimator [27]. In order to predict the change of LULC in MWW over the next 10 years, the Markov chain model and the CA-Markov model [31–34] were combined with the processed spatial inspection and modeling software TerrSet 2020 [35–36]. A good agreement is one with a kappa distribution rate greater than zero [37]. The comparison between the classification outcomes and values chosen at random is gauged by the Kappa coefficient. The categorized and ground truth images are identical if the kappa coefficient equals one. Subsequently, to boost confidence for test applications, the accuracy of LULC maps was examined. These codes allow the studied watershed's LULC to be linked to the SWAT land use database via the SWAT model. Finally, a user lookup table was prepared that identifies the SWAT code for each LULC category (2011, 2021, and 2031) to simulate the SWAT model (Table 1).

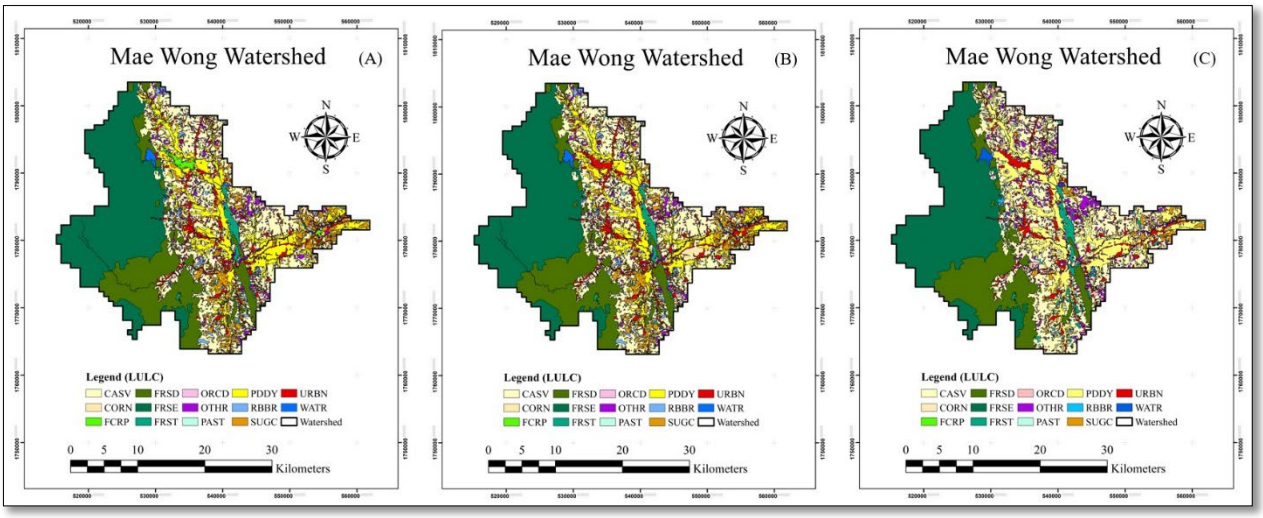

Figure 3 The LULC maps of the year 2011 (A), 2021 (B), and 2031 (C).

Table 1 SWAT model code of the land use and land cover of the MWW

No.	LULC classes	SWAT code	Year 2011		Year 2021		Year 2031	
			(km^2)	%	(km^2)	%	(km^2)	%
1	Cassava	CASV	225.83	24.55	231.60	25.18	237.43	25.81
2	Corn	CORN	11.35	1.23	13.55	1.47	15.76	1.71
3	Deciduous forest	FRSD	141.53	15.38	139.65	15.18	137.69	14.97
4	Evergreen forest	FRSE	268.16	29.15	261.47	28.42	255.65	27.79
5	Field crop	FCRP	0.67	0.07	0.82	0.09	0.95	0.10
6	Mixed forest	FRST	14.85	1.61	13.05	1.42	11.89	1.29
7	Orchard	ORCD	16.69	1.81	15.26	1.66	13.84	1.50
8	Other	OTHR	47.07	5.12	44.99	4.89	42.87	4.66
9	Paddy field	PDDY	126.89	13.79	128.98	14.02	130.23	14.16
10	Pasture	PAST	1.33	0.14	1.46	0.16	1.59	0.17
11	Rubber trees	RBBR	5.92	0.64	5.41	0.59	4.96	0.54
12	Sugarcane	SUGC	14.07	1.53	17.01	1.85	19.17	2.08
13	Urban or built-over area	URBN	37.13	4.04	38.24	4.16	39.47	4.29
14	Water	WATR	8.48	0.92	8.47	0.92	8.46	0.92
	Total		919.96	100.00	919.96	100.00	919.96	100.00

4) Model setup and simulation

The structure of the model was created to replicate the hydrological process of the watershed and assess GRSR. First, the threshold necessary for the formation of streams was carefully chosen to establish the stream definition. The slope map used in this investigation was created using a 30-meter spatial resolution DEM from the Shuttle Radar Topographic Mission database. To generate HRUs the study established the multiple slope option, taking into account various slope classes. Following that, the LULC area was divided up into HRUs using unique data pertaining to various aspects of the LULC, management, and soil qualities. HRUs improve the precision of sub-watershed loading predictions. HRUs are defined by employing DEM, LULC, and soil data. Every component of the soil water balance is calculated using HRUs, and similar HRUs would have similar hydrologic characteristics [17, 25]. For the SWAT model simulation, specific weather data is an essential requirement. Meteorological stations are required by the SWAT model both inside and outside the watershed's buffer zone to record daily data on temperature (°C), precipitation (mm), wind speed (m s^{-1}), relative humidity (percent), and solar radiation (MJ m^{-2}). This study combines meteorological data from weather monitoring stations in Kamphaeng Phet Province to simulate the hydrology of the MWW. The streamflow data were collected from observed data during the year 2020 to 2021. After that, the LULC, soil, and slope layers were overlaid, watershed HRUs were created, meteorological data was specified, and the SWAT model was run for the duration of the simulation period. The general outline of the workflow structure used in this study is in Figure 4.

5) Model calibration and validation

The tool for modeling watersheds is well-developed, reliable, and interdisciplinary. However, calibration and validation methods affect how effectively the hydrologic model predicts streamflow [25, 38–40]. Correct parameters speed up and improve model calibration, which results in lower prediction uncertainty [41], and describe comprehensive hydrological processes [42]. To quantify the calibration, validation, and sensitivity analysis of the SWAT models, the SWAT-CUP was created. The SWAT-CUP's capabilities include an automated method for doing performance analysis with greater rigor [39, 41]. The SWAT-CUP is an open-access application that links the output of the SWAT model to the SUFI-2 algorithm. The SUFI-2 accounts for all causes of uncertainty driving factors in hydrological processes [39, 43]. Sensitivity analysis establishes model output modifications in light of model modifications. This inquiry supported the automated SWAT-CUP and SUFI-2 analyses. To choose and fine-tune estimates, an auto-analysis produces suitable parameter estimates in accordance with previous data. Reflections that restrict output variations caused by input variability are provided by sensitivity analyses [39]. The p-values determine the implications while the t-stat evaluates the sensitivity [43]. Accordingly, a p-value that is close to zero is more significant while a higher t-stat value indicates a more sensitive the parameter [39]. The relative error is minimized by the practically optimal value that falls within a certain bound. A model's ability to make accurate predictions without adjusting parameter values during calibration is known as model validation [44]. The observed and simulated annual streamflow was used to calibrate (2020), and validate (2021), the effects of LULC changes on GRSR. After calibration and validation, the modeling of LULC dynamics on GRSR has been analyzed.

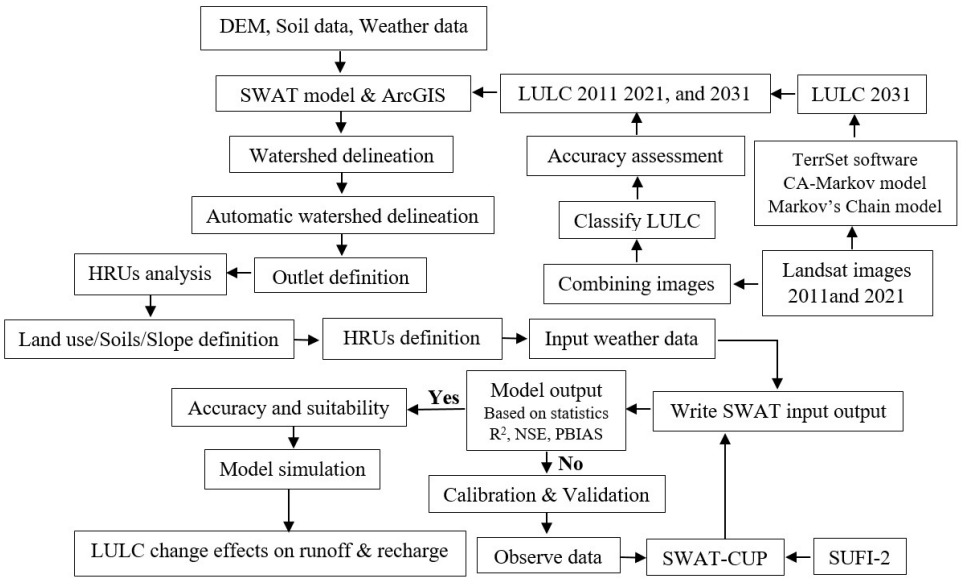

Figure 4 The overall study approach workflow design.

6) The model sensitivity analysis

ArcGIS and the SWAT model were used for the simulation and modeling of the hydrologic system. The model was simulated after preparing all of the model's inputs. Then, the sensitivity analysis was performed at the water sampling station of the Mae Wong mainstream. To improve the accuracy of results, the sensitivity analysis finds the most sensitive hydrological factors that have a substantial impact on a given model output. The monthly streamflow data simulation was performed from January 2020 to December 2020. The SUFI-2 program t-stat and p-values were used to calculate the sensitivity. The relative sensitivity in these statistics increases as the t-stat values rise. The p-values were used to fix the sensitivity implication such that the parameters become more crucial the closer the p-values are to zero. The most sensitive parameters that control the creation of streamflow were found using many more parameters before calibration and validation. Then, based on sensitivity evaluation criteria, the 16 most sensitive parameters were chosen to calibrate and validate the model's predictive abilities. In order to achieve the best simulation, the parameter values were changed one at a time while staying within reasonable limits [41]. The most sensitive parameters that were chosen and their roughly optimum values are shown with qualifications in Table 2. The extensions .hru, .gw, .mgt, .bsn, .rte, and .sol indicate the groundwater, basin, management, route, and soil HRUs that collectively make up the SWAT parameter family.

To assess model simulation performance in the watershed under changing environmental conditions brought on by numerous human-induced causes, the model was calibrated and verified. Hydrologic cycles are significantly impacted by LULC change uncertainty, which confounds the modeling results for groundwater recharge and surface runoff [5]. As for calibration, using the same parameters for calibration may not always be possible because they change when LULC changes. When LULC alterations have an impact on HRUs setups, the simulations change, this no longer has an impact on the new LULC simulation. The primary factors determining streamflow and other hydrologic components are HRUs characteristics.

In order to improve the values of sensitive parameters, simulations of each reference LULC period in the current study were calibrated using an auto-calibration technique. In order to determine whether the previously applied parameter could accurately depict the hydrologic simulation process, new parameters were also added. Nevertheless, during the LULC simulation periods in 2020, optimal values and parameter substitutions were noted irrespective of the degree of parameter similarity. As a result, the calibration for the simulation of the LULC for the year 2020 shows that the best 16 sensitive parameters were replaced with the actual simulation results and multiplied. This could help solidify strategies for the development of land and water resources.

Table 2 Optimized settings and sensitive model calibration parameters for the LULC 2020 simulation

No.	Parameter code	Parameter name	Input file	Range	Optimized value
1	CANMX	Maximum canopy storage	.hru	10–100	48.651
2	ESCO	Soil evaporation compensation coefficient	.hru	0–1	0.076
3	EPCO	Plant uptake compensation factor	.hru, bsn	0–1	0.861
4	SURLAG	Surface runoff lag coefficient	.bsn	0–24	13.854
5	ALPHA_BF	Base flow recession constant	.gw	0.01–1	0.261
6	SHALLST	Initial depth of the shallow aquifer	.gw	0–5000	412.852
7	GWQMN	Threshold depth of shallow water aquifer	.gw	0–2	0.823
8	GW_DELAY	Delay time for aquifer recharge	.gw	0–350	201.360
9	GW_REVAP	Revap coefficient	.gw	0.02–0.2	0.081
10	GW_SPYLD	Specific yield of the shallow aquifer	.gw	0-0.4	0.214
11	CN2	Moisture condition II curve number	.mgt	0.02–0.2	0.072
11	CH_K2	Effective hydraulic conductivity in the main channel	.rte	0.01–150	98.637
13	CH_N(2)	Manning's "n" value for the main channel.	.rte	-0.01-0.3	0.117
14	SOL_AWC	Available water capacity	.sol	0.5–0.5	0.378
15	SOL_K	Saturated hydraulic conductivity	.sol	0.5–0.5	-0.419
16	SOL_ZMX	Maximum rooting depth in the soil	.sol	0.5–1	0.788

7) Estimation of model predictive accuracy

The SWAT-CUP was used to assess statistical indications in order to determine the optimal parameter. The dependability of forecasts in comparison to experimental values of SWAT model performance was determined using the coefficient of determination (R^2), NSE, and percent bias (PBIAS). The percentage of variance used by R^2 shows correlations between predicted and actual values. R^2 is a measure of how well or poorly data are presented, and values near 0 and 1 indicate the opposite. The NSE evaluates the hydro-graphs' overall agreement and prediction ability. The NSE should be close to 1 for satisfactory model performance. PBIAS measures the consistency between simulated and actual data. On the basis of a range of values for R^2, NSE, and PBIAS, the model performance ratings were assessed.

Results and discussion

1) Evaluating the streamflow performance of hydrological models

The SWAT-CUP application with the SUFI-2 set of rules has been employed for calibration, validation, and uncertainty assessment of the SWAT output. The model was calibrated for this study's many independent calibration time steps to improve the realism of the simulation results. The statistically significant model performance over time intervals was evaluated using the R^2, NSE, and PBIAS measures. If the statistical criteria R^2, NSE, PBIAS, and graphic suitability are met, the hydrology is deemed to be accurately replicated and representative of the watershed. The calibration period of the SWAT model was in the year 2020, and its validation period was in the year 2021. The model's output demonstrated that the R^2, NSE, and PBIAS statistical values, which simulate monthly streamflow, were 0.97, 0.89, and 4.3%, respectively during the calibration time steps of the year 2020 land use simulation. The model was validated with observed streamflow data in the year 2021 without further adjusting calibration parameters. A regular correlation between rainfall and runoff was observed, and the SWAT overall performance for the year 2021 LULC simulation during validation was 0.95, 0.87, and -3.2% for R^2, NSE, and PBIAS, respectively. As depicted in Figure 5, the results were in good agreement with actual and simulated streamflow data, according to the hydrographs. The chosen statistical performance indicators demonstrate that the calibration and validation periods have a good agreement and are within acceptable ranges. According to the scattered plot of the observed and simulated streamflow, the best-fit line's correlation coefficient of 0.97 during calibration for the year 2020, in Figure 6A, and 0.95 during validation time steps is observed for the year 2021 land use periods, in Figure 6B, respectively. For each calibration and validation time step, the results of the statistical performance evaluation have been statistically accurate. According to the statistical results, objective functions were suitable for model evaluation and comparable to other worldwide studies for each calibration and validation time step [1, 20–22, 45–47]. Total precipitation, soil water storage, and evaporation all affect surface runoff. The most increased flows in September, August, and July were 132.45, 114.41, and 98.47 $m^3\ s^{-1}$, and the lowest decreased flows in January, December, and February were 12.23, 23.01, and 24.36 $m^3\ s^{-1}$, respectively. As a result, it was determined that the simulated SWAT model's applicability was reasonably acceptable in the MWW and agreed with regional and international studies.

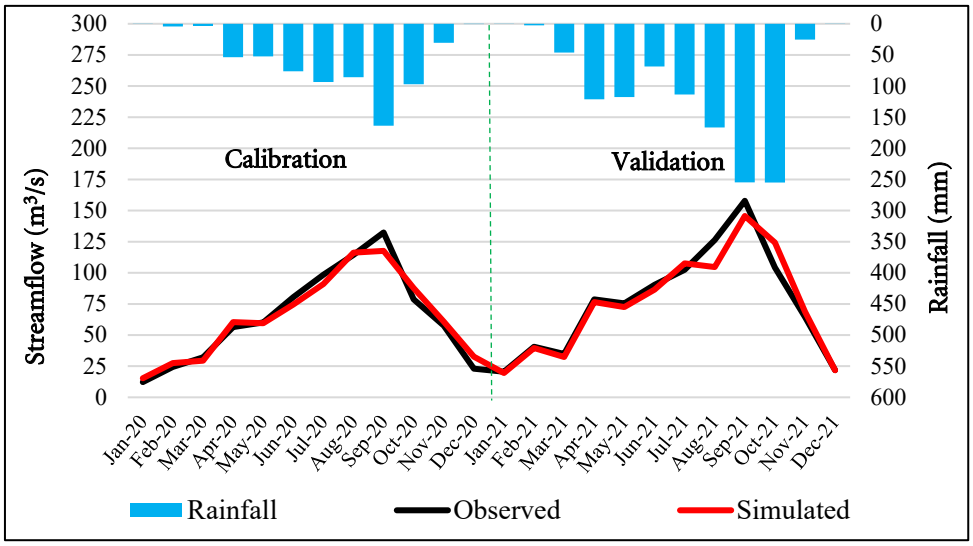

Figure 5 Hydrograph of measured and simulated flow during calibration 2020, and validation 2021.

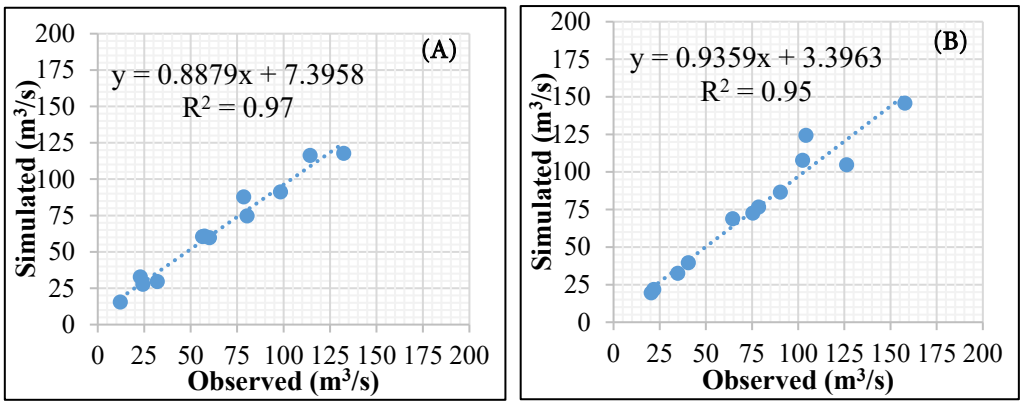

Figure 6 Scatter plot of measured and simulated flow during calibration in the year 2020 (A), and validation in the year 2021 (B).

2) Effects of LULC change

As improve the long-term viability of water resources in every basin, ongoing research and the creation of context-specific groundwater recharge models are vital. The understanding of LULC change will enable planners and policy-makers to lessen negative effects in watershed hydrology. In the overall watershed, the forest covers have undergone deforestation and decreased (evergreen, deciduous, and mixed forest), has been transformed into cassava, sugarcane, and paddy field, and have increased over the last two decades (2011, 2021, and 2031). The corn, urban or built-over area, and field crop were augmented by 0.240%, 0.120%, and 0.016% from the year 2011 to 2021 and 0.480%, 0.254%, and 0.030% from the year 2011 to 2031. The other area, orchard, and rubber trees have proven to continuously decrease by 0.226%, 0.155%, and 0.055% from the year 2011 to 2021, 0.230%, 0.154%, and 0.049% from the year 2021 to 2031, and 0.456%, 0.309%, and 0.104% from the year 2011 to 2031. An increase in agricultural lands (sugarcane, cassava, corn, paddy field, field crop, and pasture), and urban or built-over area results in a reduction of decrease of most of the forested areas (Table 3). Assessment of LULC over a long time confirmed continuous agricultural activity, numerous anthropogenic activities are associated with socioeconomic environments, and deforestation reduced forested areas.

The effects showed significant variations in LULC that occurred from the year 2011 to 2031. LULC disturbs water yields by reducing infiltration and increasing surface runoff in the watershed. The goal of increasing cultivation is to produce a crop at the expense of forest areas. This makes the land more vulnerable to erosion and the sedimentation of waterways and reservoirs. This is due to decreasing plant-available water, loss of nutrients, deterioration of the soil, loss of rich topsoil, and fall in organic matter, which all result in lower agricultural yields.

The need for more agricultural lands grows along with population growth, which is why farming products are grown. Human activities have significantly changed the LULC changes in the MWW. Due to agriculture's impact on water bodies in the ecosystem and land surfaces, there is a change in vegetation and forest areas. The agricultural land use practice encourages more surface runoff than infiltration. Therefore, LULC change has a significant impact on spatiotemporal evaluation for socio-economic and environmental development. The findings are in agreement with studies conducted by [3, 9, 26, 48-51].

3) Effects of the LULC change on surface runoff

In watershed hydrology, LULC modification typically causes large changes in flood peak and infiltration characteristics, affecting the watershed's total hydrological condition. To estimate the water balance, it is crucial to evaluate the spatiotemporal variability, the impact, and the implications of LULC changes. With well-calibrated model simulation, the computational reliability of hydrological model simulation increases [1]. In the present study, the impact of LULC changes on GRSR, the SWAT model in the current study was first calibrated using the LULC map from the year 2011, and then updated to the year 2021 and the year 2031. For the first LULC in the year 2011 period, the watershed has a total mean annual value of actual evapotranspiration of 314.57 mm, surface runoff of 106.56 mm, groundwater of 201.63 mm, recharge of 189.31 mm, lateral flow of 85.78 mm, and water yield of 394.65 mm. The simulated annual water balances indicated that actual evapotranspiration loses 24.86% of the yearly precipitation and 75.41% of the rainfall in the watershed contributes to the streamflow during the simulation period. The average annual contribution of groundwater relative to rainfall is 35.54%. Therefore, 39.61% of precipitation is lost as groundwater recharge.

Table 3 LULC change of MWW from the year 2011 to 2031

LULC classes	LULC 2011		LULC 2021		LULC change 2011-2021		LULC 2031		LULC change 2021-2031		LULC change 2011-2031	
	km²	%	km²	%	km²	%	km²	%	km²	%	km²	%
Cassava	225.83	24.55	231.60	25.18	5.775	0.628	237.43	25.81	5.830	0.634	11.605	1.261
Corn	11.35	1.23	13.55	1.47	2.204	0.240	15.76	1.71	2.210	0.240	4.414	0.480
Deciduous forest	141.53	15.38	139.65	15.18	-1.880	-0.204	137.69	14.97	-1.960	-0.213	-3.840	-0.417
Evergreen forest	268.16	29.15	261.47	28.42	-6.689	-0.727	255.65	27.79	-5.820	-0.633	-12.509	-1.360
Field crop	0.67	0.07	0.82	0.09	0.147	0.016	0.95	0.10	0.130	0.014	0.277	0.030
Mixed forest	14.85	1.61	13.05	1.42	-1.798	-0.195	11.89	1.29	-1.160	-0.126	-2.958	-0.322
Orchard	16.69	1.81	15.26	1.66	-1.425	-0.155	13.84	1.50	-1.420	-0.154	-2.845	-0.309
Other area	47.07	5.12	44.99	4.89	-2.078	-0.226	5.00	4.66	-2.120	-0.230	-4.198	-0.456
Paddy field	126.89	13.79	128.98	14.02	2.085	0.227	130.23	14.16	1.250	0.136	3.335	0.363
Pasture	1.33	0.14	1.46	0.16	0.128	0.014	1.59	0.17	0.130	0.014	0.258	0.028
Rubber trees	5.92	0.64	5.41	0.59	-0.506	-0.055	4.96	0.54	-0.450	-0.049	-0.956	-0.104
Sugarcane	14.07	1.53	17.01	1.85	2.943	0.320	19.17	2.08	2.160	0.235	5.103	0.555
Urban or built-over area	37.13	4.04	38.24	4.16	1.107	0.120	39.47	4.29	1.230	0.134	2.337	0.254
Water	8.48	0.92	8.47	0.92	-0.009	-0.001	8.46	0.92	-0.010	-0.001	-0.019	-0.002
Total	919.96	100.00	919.96	100.00	-	-	919.96	100.00	-	-	-	-

Surface runoff is the main component of streamflow and is crucial for determining the potential for groundwater recharge. The LULC is an important aspect of the surface runoff process that influences groundwater flow, infiltration rate, soil water content, and water yield. Surface runoff is the main streamflow contributor to aquifers in watershed hydrology. The simulated total average surface runoff in the year 2011, 2021, and 2031 was 106.65 mm, 145.66 mm, and 156.88 mm, respectively. The results of the LULC transformation indicate that surface runoff tends to continue in-creasing. The excess water flows can be stored and used during low flow conditions. The simulated streamflow accounts for the LULC change scenarios classified into the wet period (July to October) and dry period (November to December, and January to March). Surface runoff as a result was quite high during the rainy season and relatively low during the dry period. This analysis demonstrated that the expansion of agricultural lands results in direct runoff during the wet period. If suitable control measures are not taken, the increase in runoff could have wide-ranging effects on rising soil erosion and sedimentation. Additionally, it degrades low-lying plains, natural riverbanks, and agricultural lands by removing the top layer of useful soil. These crop yields are decreased, which causes food insecurity and sediment to enter downstream, shortening the lifespan of service downstream systems. According to the surface runoff chart, sub-watersheds with heavy rainfall have an excessive runoff. The surface runoff map suggests that sub-watersheds with high rainfall correspond to extreme runoff, as in Figures 7A, 7B, and 7C, respectively. The sub-watershed numbers 5 in the year 2011, sub-watershed numbers 4 and 5 in the year 2021, and sub-watershed numbers 4, 5, and 7 in the year 2031, were highly attributed to the surface runoff of 107.07 mm to 135.86 mm annually. The lowland elevation areas see high yearly surface runoff because water cannot penetrate the soil surface and most of the area is used for agriculture. In flat-sloping regions of lowlands, surface runoff is also higher on forestland, resulting in human activities in the watershed and significant driving factors for LULC change. These findings agree with other similar efforts [2, 7, 10, 13–14, 46].

4) Effects of land use and land cover (LULC) change on groundwater recharge

An essential hydrologic cycle for maintaining aquifers refilled by precipitation is groundwater recharge. Therefore, by boosting recharge and reducing surface runoff, the optimal management options could help preserve stream biotas within the ecosystems. The best management strategies decrease surface runoff and increase groundwater recharge, which lowers erosion as in-stream sediment loads decline. For example, surface runoff was reduced when agricultural land was returned to its natural state. Additionally, it lowered in-stream sediment loads as a result of less erosion. Furthermore, the LULC change had an impact on surface runoff, which increased as interception fell, and the amount of forest cover decreased. Poor land-use practices change the structure and porosity of the soil, lower the rate of infiltration, and increase surface runoff. Intensive agricultural methods, however, that exposed dense soils to erosion by eliminating plant covers, reduced groundwater recharge in the aquifer.

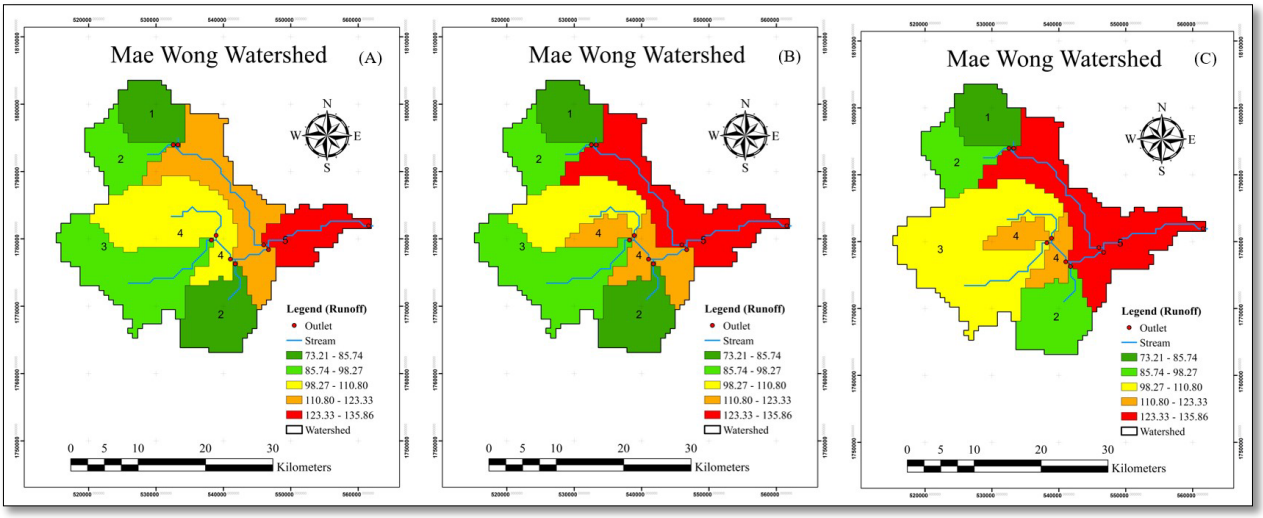

Figure 7 Spatiotemporal patterns of surface runoff during 2011 (A), 2021 (B), and 2031 LULC simulation periods (C).

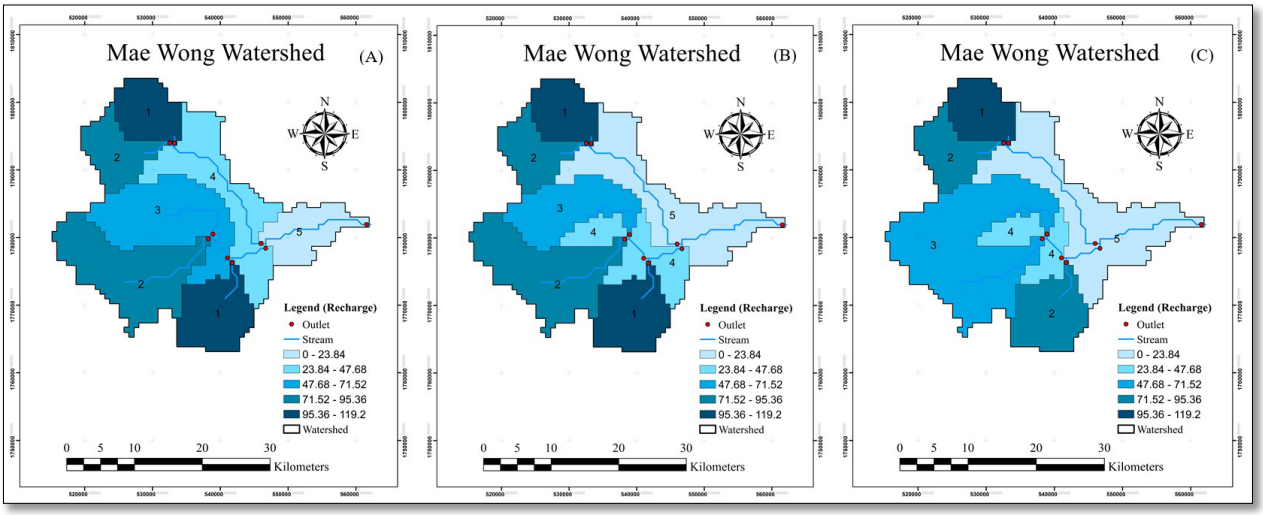

Figure 8 Spatiotemporal pattern of groundwater recharge in the year 2011 (A), 2021 (B), and 2031 reference LULC periods (C).

The LULC has a significant impact on groundwater recharge, and it is crucial to comprehend how it interacts with rising levels of natural and human activity. According to the calibrated SWAT model for the LULC reference periods in the year 2011, 2021, and 2031, the average simulated rainfall is expected to be 189.31 mm, 167.35 mm, and 156.88 mm, respectively. At the sub-watershed scale, groundwater recharge varies from 0 to 119.20, 0 to 109.55, and 0 to 98.20 mm for the year 2011, 2021, and 2031, respectively. The sub-watershed numbers 1 and 9 in the year 2011, sub-watershed numbers, 1 and 9 in the year 2021, and sub-watershed numbers 1 in the year 2031, were attributed to high groundwater recharge. The sub-surface infiltration of alluvial deposits is possible in rangeland and sandy, loamy soil. The spatial pattern of GRSR showed the direct effects of surface runoff reducing the ground-water recharge rate in 2011, as in Figures 8A, 8B, and 8C, respectively. The agricultural sub-watersheds show the lowest recharge levels. The decrease in streamflow is linked to less infiltration, recharge conditions, and lower surface runoff as a result of more forestland, which raises the soil is water-holding capacity of the soil. High evapotranspiration may also contribute to the reduction in groundwater recharge.

The temporal variation of groundwater recharge showed that the highest value occurred during the wet period (July to October). The LULC simulation scenarios dry period has indicated lowering responses of ground-water recharge during the dry periods (November to December, and January to March). The main reason for reducing the average annual groundwater recharge is the long dry period. The findings revealed increasing wet periods, and lower dry periods due to the alteration of vegetation cover in agricultural lands over study periods, including the reduction of forest area, which

has been converted to agricultural land, it has resulted in a decrease in the rate of water infiltration through surface water into groundwater. Similar efforts in many reported that field crop, orchard, and urban development increased runoff and decreased recharge when agricultural expansion reduced forest cover. As a result, flooding during the wet season and a reduction in low flow during the dry season [3, 7, 13, 52–53]. Therefore, a possible recurring hydrological drought was shown by the lower recharge caused by the LULC shift. Knowing the flow regimes of the wet and dry periods in the watershed requires an understanding of how it affects GRSR. Hence, efforts should be made to improve watershed management techniques in order to make the best use of available resources for the socio-economic growth of the country. In order to preserve the ecological and riverine ecosystems, sustainable land and water management is crucial.

Conclusion

In this study, three reference scenarios in the MWW of Thailand were used to assess the spatiotemporal effects and implications of LULC variations on GRSR. The LULC changes derived from satellite images showed an increase in agricultural lands was 2.72% (cassava, corn, field crop, paddy field, pasture, and sugarcane), and a decline in forestland was 2.10% (deciduous forest, evergreen forest, and mixed forest) from the year 2011 to 2031 due to human activity and population growth. The findings indicate that the vast agricultural operations in the watershed have changed, resulting in a reduction of forestland via deforestation of the forests. The findings imply that the watershed GRSR is significantly impacted by LULC changes. The calibrated model confirmed that variations in LULC resulted in an increase in runoff and a decrease in replenishment. The study carefully examined how LULC changes, which are mostly brought about by the spread of intensive agriculture and the removal of forestlands, affected GRSR. Therefore, developing scenarios for watershed management is crucial to reducing the adverse effects of LULC changes on GRSR. Planners and decision-makers of water resource projects must give serious consideration to the LULC response. It was discovered as a result that offering insights into calibrated out-comes aids in the development of a detailed plan for upcoming management strategies on watershed hydrology. As groundwater is the primary source of available freshwater, sustainable development goals are directly tied to how it is used, managed, and sustained. Future studies should investigate the impact of LULC change on rock layers, infiltration and percolation rate, and ground water level, which will ultimately help to develop a plan for sustainable use of the watershed management.

Acknowledgements

The authors are thankful to the Kamphaeng Phet Rajabhat University for their support during this study. We would like to express our gratitude to Professor Dr.Nipon Thangtham and Professor Dr.Kasem Chankaew at Kasetsart University, who kindly gave suggestions and knowledge. Again, we would like thank everyone for participating in this study.

References

[1] Mengistu, T.D., Chung, I.M., Kim, M.G., Chang, S.W., Lee, J.E. impacts and implications of land use land cover dynamics on groundwater recharge and surface runoff in East African watershed. Journal of Water, 2022, 14(13), 2068.

[2] Guzha, A.C., Rufino, M.C., Okoth, S., Jacobs, S., Nybrega, R.L.B. Impacts of land use and land cover change on surface runoff, discharge and low flows: Evidence from East Africa. Journal of Hydrology, Regional Studies 2018, 15, 49–67.

[3] Banchongsak, F., Wilailak, S., Nopparat, C., Pimprapai, K., Nares, K., Siraprapa, M., Saksri, S., Bunchongsri, P. Application of mathematical model with geoinformatics system for prediction of land use change in Pong Nam Ron Sub-watershed, Khlong Lan District, Kamphaengphet Province. Srinakharinwirot University. Journal of Science and Technology 2022, 14(27), 119–130.

[4] Coelho, V.H.R., Montenegro, S., Almeida, C.N., Silva, B., Oliveira, L.M., Gusmro, A.C.V., Freitas, E.S., Montenegro, A.A.A. Alluvial groundwater recharge estimation in semi-arid environment using remotely sensed data. Journal of Hydrology, 2017, 548, 1–15.

[5] Mensah, J.K., Ofosu, E.A., Yidana, S.M., Akpoti, K., Kabo-bah, A.T. Integrated modeling of hydrological processes and groundwater recharge based on land use land cover, and climate changes: A systematic review. Journal of Environmental Advances, 2022, 8, 100224.

[6] Pavelic, P. Groundwater availability and use in Sub-Saharan Africa: A review of 15 countries, International Water Management Institute (IWMI): Colombo, Sri Lanka, 2012, ISBN 9789290907589.

[7] Gessesse, A.A., Melesse, A.M., Abera, F.F., Abiy, A.Z. Modeling hydrological responses to land use dynamics, Choke, Ethiopia. Journal of Water Conservation Science and Engineering, 2019, 4, 201–212.

[8] Mengistu, T.D., Chung, I.-M., Chang, S.W., Yifru, B.A., Kim, M.G., Lee, J., Ware, H.H., Kim, I.H. Challenges and prospects of advancing groundwater research in Ethiopian Aquifers: A review. Journal of Sustainability, 2021, 13, 11500.

[9] Demissie, F., Yeshitila, K., Kindu, M., Schneider, T. Land use/land cover changes and their causes in Libokemkem District of South Gonder, Ethiopia. Journal of Remote Sensing Applications: Society and Environment, 2017, 8, 224–230.

[10] Banchongsak, F., Wilailak, S., Nopparat, C., Nares, K., Sineepa, B. Land use changes of head watershed area on streamflow, suspended sediment and water quality in Khlong Lan Watershed, Kamphaeng Phet Province. Burapha Science Journal, 2019, 24, 2, 532–549.

[11] Getu Engida, T., Nigussie, T.A., Aneseyee, A.B., Barnabas, J. Land use/land cover change impact on hydrological process in the Upper Baro Basin, Ethiopia. Journal of Applied and Environmental Soil Science, 2021, 6617541.

[12] Scanlon, B.R., Reedy, R.C., Stonestrom, D.A., Prudic, D.E., Dennehy, K.F. Impact of land use and land cover change on groundwater recharge and quality in the southwestern US. Journal of Global Change Biology, 2005, 11, 1577–1593.

[13] Gashaw, T., Tulu, T., Argaw, M., Worqlul, A.W. Modeling the hydrological impacts of land use/land cover changes in the Andassa watershed, Blue Nile Basin, Ethiopia. Journal of Science of the Total Environment, 2018, 1394–1408.

[14] Jin, X., Jin, Y., Yuan, D., Mao, X. Effects of land-use data resolution on hydrologic modeling a case study in the upper reach of the Heihe River, Northwest China. Journal of Ecological Modelling, 2019, 404, 61–68.

[15] Suryavanshi, S., Pandey, A., Chaube, U.C. Hydrological simulation of the Betwa River basin (India) using the SWAT model. Hydrological Sciences Journal, 2017, 62, 960–978.

[16] Zewdie, M., Worku, H., Bantider, A. Temporal dynamics of the driving factors of urban landscape change of Addis Ababa during the past three decades. Journal of Environmental Management, 2018, 61, 132–146.

[17] Arnold, J.G., Srinivasan, R., Muttiah, R.S., Williams, J.R. Large area hydrologic modeling and assessment part I: Model development. Journal of the American Water Resources Association, 1998, 34, 73–89.

[18] Santhi, C., Allen, P.M., Muttiah, R.S., Arnold, J.G., Tuppad, P. Regional estimation of base flow for the conterminous united states by hydrologic landscape regions. Journal of Hydrology, 2008, 351, 139–153.

[19] Ghoraba, S.M. Hydrological modeling of the simly dam watershed (Pakistan) using GIS and SWAT model. Alexandria Engineering Journal, 2015, 54, 583–594.

[20] Astuti, I.S., Sahoo, K., Milewski, A., Mishra, D.R. Impact of land use land cover (LULC) change on surface runoff in an increasingly urbanized tropical watershed. Journal of Water Resources Management, 2019, 33, 4087–4103.

[21] Chen, Y., Niu, J., Sun, Y., Liu, Q., Li, S., Li, P., …, Li, Q. Study on streamflow response to land use change over the upper reaches of Zhanghe Reservoir in the Yangtze River Basin. Journal of Geoscience Letters, 2020, 7, 6.

[22] Chen, Y., Nakatsugawa, M. Analysis of changes in land use/land cover and hydrological processes caused by earthquakes in the Atsuma River Basin in Japan. Journal of Sustainability, 2021, 13, 13041.

[23] Qiu, W., Ma, T., Wang, Y., Cheng, J., Su, C., Li, J. Review on status of groundwater database and application prospect in deep-time digital earth plan. Journal of Geoscience Frontiers, 2022, 13, 101383.

[24] Sime, C.H., Demissie, T.A., Tufa, F.G. Surface runoff modeling in Ketar Watershed, Ethiopia. Journal of Sedimentary Environments, 2020, 5, 151–162.

[25] Neitsch, S.L., Arnold, J.G., Kiniry, J.R., Williams, J.R. Soil and water assessment tool theoretical, documentation version 2009, Texas Water Resources Institute: Temple, TX, USA, 2011, 543.

[26] Woldesenbet, T.A., Elagib, N.A., Ribbe, L., Heinrich, J. Hydrological responses to land use/cover changes in the source region of the Upper Blue Nile Basin, Ethiopia. Journal of Science of the Total Environment, 2017, 575, 724–741.

[27] Ghalehteimouri, K.J., Shamsodini, A., Mousavi, M.N., Binti, F., Ros, C., Khedmatzadeh, A. Predicting spatial and decadal of land use and land cover change using integrated cellular automata Markov chain model based scenarios (2019-2049) Zarrinй-Rūd River Basin in Iran. Journal of Environmental Challenges, 2021, 6, 100399.

[28] Neitsch, S.L., Arnold, J.G., Kiniry, J.R., Williams, J.R. Soil and water research laboratory - Agricultural research service, blackland research center, documentation version 2011, Texas Water Resources Institute Technical Report No. 406, 2011, 77843–2118.

[29] Gassman, P.W., Reyes, M.R., Green, C.H., Arnold, J.G. The soil and water assessment tool: Historical development, applications, and future research directions. Journal of Transactions of the ASABE, 2007, 50, 1211–1250.

[30] Leta, M.K., Demissie, T.A., Trдnckner, J. Hydrological responses of watershed to historical and future land use land cover change dynamics of Nashe Watershed, Ethiopia. Journal of Water, 2021, 13, 2372.

[31] Guan, D., Li, H., Inohae, T., Su, W., Nagaie, T., Hokao, K. Modeling urban land-use change by the integration of cellular automaton and markov model. Journal of Ecological Modelling, 2011, 222(20-22), 3761-3772.

[32] Sinha, P., Kimar, L. Markov land cover change modeling using pairs of time-series satellite images. Journal of Photogrammetric Engineering and Remote Sensing, 2013, 79(11), 1037–1051.

[33] Varga, O.G., Pontious Jr., R.G., Singh, S.K., Szabo, S. Intensity analysis and the fig of merit's components for an assessment of cellular automata-markov simulation model. Journal of Ecological Indicators, 2019, 101, 933–942.

[34] Mohamed, M., Brijesh, K.Y., Mwemezi, J.R., Isaac, L., Sekela, T. Analysis of land use and land-cover pattern to monitor dynamics of Ngorongoro world heritage site (Tanzania) using hybrid cellular automata-markov model. Journal of Current Research in Environmental Sustainability, 2022, 4, 100126.

[35] Eastman, J.R. Idrisi Taiga, a guide to GIS and image processing. Clark University, 2009.

[36] Li, S., Jin, B., Wei, X., Jiang, Y., Wang, J. Using CA-Markov model to model the spatiotemporal change of land use/cover in Fuxian Lake for decision support. International workshop on spatiotemporal computing, ISPRS annals of the photogrammetry, Remote Sensing and Spatial Information Sciences, Virginia, United States, 2015, 13–15 July.

[37] Anthony, J., Viera, A.J.V. The kappa statistic. Journal of the American Medical Association, 1992, 268, 2513–2514.

[38] Setegn, S.G., Srinivasan, R., Melesse, A.M., Dargahi, B. SWAT model application and prediction uncertainty analysis in the Lake Tana Basin, Ethiopia. Journal of Hydrological Processes, 2009, 24, 357–367.

[39] Abbaspour, K.C., Rouholahnejad, E., Vaghefi, S., Srinivasan, R., Yang, H., Klшve, B. A continental-scale hydrology and water quality model for Europe: Calibration and uncertainty of a high-resolution large-scale SWAT model. Journal of Hydrology, 2015, 524, 733–752.

[40] Kouchi, D.H., Esmaili, K., Faridhosseini, A., Sanaeinejad, S.H., Khalili, D., Abbaspour, K.C. Sensitivity of calibrated parameters and water resource estimates on different objective functions and optimization algorithms. Journal of Water, 2017, 9, 384.

[41] Arnold, J.G., Moriasi, D.N., Gassman, P.W., Abbaspour, K.C., White, M.J., Srinivasan, R., …, Jha, M.K. SWAT: Model use, calibration, and validation. Journal of Transactions of the ASABE, 2012, 55, 1491–1508.

[42] Meaurio, M., Zabaleta, A., Uriarte, J.A., Srinivasan, R., Antigьedad, I. Evaluation of SWAT models performance to simulate streamflow spatial origin. The case of a small-forested watershed. Journal of Hydrology, 2015, 525, 326–334.

[43] Abbaspour, K.C. Calibration of hydrologic models: When is a model calibrated? In proceedings of the MODSIM05: International congress on modelling and simulation: advances and applications for management and decision making, Melbourne, Australia, 2005, 12–15, 2449–2455

[44] Refsgaard, J.C., Knudsen, J. Operational validation and intercomparison of different types of hydrological models. Journal of Water Resources Research, 1996, 32, 2189-2202.

[45] Thomas, C.C.H., Kwong, F.A.L. Effects of land use change on sediment and water yields in Yang Ming Shan National Park, Taiwan. Environments, 2015, 2, 32–42.

[46] Gyamfi, C., Ndambuki, J.M., Anornu, G.K., Kifanyi, G.E. Groundwater recharge modelling in a large-scale basin: An example using the SWAT hydrologic model. Journal of Modeling Earth Systems and Environment, 2017, 3, 1361–1369.

[47] Mengistu, A.G., van Rensburg, L.D., Woyessa, Y.E. Techniques for calibration and validation of SWAT model in data scarce arid and semi-arid catchments in South Africa. Journal of Hydrology: Regional Studies, 2019, 25, 100621.

[48] Zeleke, G., Hurni, H. Implications of land use and land cover dynamics for mountain resource degradation in the Northwestern Ethiopian highlands. Journal of Mountain Research and Development, 2001, 21, 184–191.

[49] Bewket, W., Sterk, G. Dynamics in land cover and its effect on stream flow in the Chemoga watershed, Blue Nile Basin, Ethiopia. Journal of Hydrological Processes, 2005, 19, 445–458.

[50] Gessesse, B., Bewket, W., Brдuning, A. Model-based characterization and monitoring of runoff and soil erosion in response to land use/land cover changes in the Modjo Watershed, Ethiopia. Journal of Land Degradation and Development, 2015, 26, 711–724.

[51] Moges, D.M., Bhat, H.G. An insight into land use and land cover changes and their impacts in Rib Watershed, north-western highland Ethiopia. Journal of Land Degradation and Development, 2018, 29, 3317–3330.

[52] Banchongsak, F., Bualert, S., Dampin, N., Thangtham, N. Dynamic modeling of water storage capacity for the dilution of waste water of land utilization in the Upper Tha Chin Watershed, Thailand, Journal of EnvironmentAsia, 2017, 10 (2), 33–42.

[53] Birhanu, A., Masih, I., van der Zaag, P., Nyssen, J., Cai, X. Impacts of land use and land cover changes on hydrology of the Gumara Catchment, Ethiopia. Journal of Physics and Chemistry of the Earth, 2019, 112, 165–174.